Quantitative Compressibility Effects in Thermal Elastohydrodynamic Circular Contacts

W. Habchi[1,2*] and S. Bair[2]

[1] Lebanese American University, Dep. of Ind. & Mech. Eng., Byblos, Lebanon
[2] G.W. Woodruff School of Mech. Eng., Center for High Pressure Rheology, Georgia Institute of Technology, Atlanta, GA 30332-0405

*At the time this work was done, the first author was holding a visiting scholar position at Georgia Institute of Technology

Abstract

This paper investigates the effects of lubricant compressibility on the film-forming performance of thermal elastohydrodynamic lubricated (EHL) circular contacts. Numerical film thickness predictions using the classical Dowson and Higginson relationship are compared to those that would be obtained using a more realistic compressibility model, all other parameters kept unchanged. This allows an isolation of the realistic compressibility effects on the film-forming performance. For realistic predictions, the authors consider two model liquids from the 1953 report of the ASME Research Committee on Lubrication, the most and the least compressible. The compressibility of these liquids is modeled using the Tait equation of state (EoS) while all other transport properties are kept unchanged for the sake of isolating compressibility effects. In addition, the same typical generalized-Newtonian behavior is assumed for both model liquids. The results reconfirm the well-known observations that minimum film thickness is very little affected by lubricant compressibility while central film thickness decreases linearly with the increase in volume compression of the lubricant. It is also observed that the relative errors on central film thicknesses induced by the use of the Dowson and Higginson relationship for compressibility increase with load and temperature and are very little affected by mean entrainment speed. Compressibility is shown to be a significant source of error in film-derived measurements of pressure-viscosity coefficients especially at high temperature. The thermodynamic scaling which provides an accurate and consistent framework for the correlation of the thermophysical properties of liquids with temperature and pressure requires an accurate equation of state. In brief, this paper highlights the importance of using realistic transport properties modeling based on thermodynamic scaling for an accurate numerical prediction of the performance of EHL contacts.

Keywords: Lubricant compressibility, Thermal elastohydrodynamic lubrication, Circular contacts, generalized-Newtonian lubricant

1. Introduction

The effect of lubricant compressibility on the performance of elastohydrodynamic lubricated (EHL) contacts has earned very little attention from the tribological community. This is because from the early pioneering work of Dowson and Higginson [1], Hamrock and Dowson [2][3] or Kweh et al. [4] it was noted that compressibility has a minor effect on minimum film thickness in elastohydrodynamic lubricated contacts. The effect was more noticeable on central film thickness which is significantly reduced with lubricant compressibility.

To the authors' knowledge, the only work that attempted to quantify the effect of realistic compressibility on film thickness in EHL was that of Venner and Bos [5]. These authors employed the Jacobson and Vinet [6] isothermal equation of state which provides a better prediction of lubricant compressibility at high pressures than the widely used Dowson and Higginson [7] relationship. They found that the central film thickness decreases linearly with the increase in compression of the lubricant (induced by the use of the Jacobson and Vinet relationship) while little effect was observed on minimum film thickness. This important observation allowed engineers to correct their film thickness predictions which are derived from numerical simulations employing the Dowson and Higginson relationship. However, two decades later, the Dowson and Higginson relationship for compressibility is still the most widely used EoS in numerical modeling of EHL contacts. This is in part due to the fact that the Jacobson and Vinet relationship has a somewhat inconvenient form for EHL solvers as it provides pressure as a function of density and cannot be easily inverted. In addition, although this equation can be more accurate than the Dowson and Higginson relationship, it has some shortcomings which prevent it from predicting a realistic physical based pressure-temperature dependence of density as shall be discussed in the following section.

The work of Venner and Bos [5] was based on an isothermal Newtonian analysis using hypothetical lubricant transport properties. The current paper revisits the effects of compressibility on film thickness in EHL circular contacts while alleviating the simplifying assumptions employed in [5]. In fact, both thermal and generalized-Newtonian effects are considered. In addition, realistic rheological models are used. These are based on experimental data describing the dependence of viscosity on pressure, temperature and shear stress as well as the dependence of density on pressure and temperature. In addition, the equation of state (EoS) describing the latter has a convenient form for an easy incorporation into EHL solvers. Density scaling provides a precise and consistent correlation of the thermophysical properties of the liquid [8] and such correlations are essential to quantitative EHL. Density scaling requires an accurate EoS.

This is not the first attempt to use such realistic rheological models. In fact, the authors have previously employed these and obtained an accurate prediction of film thickness as well as friction in EHL contacts over a wide range of operating conditions [9] [10]. It is noteworthy to mention that these numerical predictions were validated against experiments without any alteration of the rheological parameters used in the numerical model. The idea behind the current

work is to use this validated numerical framework to compare its predictions with those obtained using the classical Dowson and Higginson relationship, all other parameters kept unchanged. This would allow an isolation of the effects of realistic compressibility on the performance of EHL contacts.

2. Compressibility in EHL

The treatment of compressibility in EHL has a similar history as the treatment of piezoviscosity. For the earliest numerical studies, a simple isothermal EoS was employed [7] for the qualitative film thickness solutions which famously established the field. This EoS is commonly known as the Dowson and Higginson equation:

$$\rho = \rho_0(T)\left[1+\frac{0.6p}{1+1.7p}\right],\ p \text{ in GPa} \qquad (1)$$

This empirical formula was obtained from measurements for a mineral oil at pressures to 350 MPa at a single temperature [7]. A limit of compression was mentioned but not observed.

In EHL, the compressibility $(-\rho^{-1}\partial\rho/\partial p)$ is assumed to be universally temperature independent and the complete EoS has (for example, [11]) been

$$\rho = \rho_0(T_R)\left[1+\frac{0.6p}{1+1.7p}-0.65\times10^{-3}(T-T_R)\right],\ p \text{ in GPa, } T \text{ and } T_R \text{ in K} \qquad (2)$$

This EoS served the needed purpose of demonstrating the effect of liquid compressibility on the film shape just as the simple pressure-viscosity models demonstrated the dependence of film thickness on the pressure-viscosity coefficient. However, just as the simple piezoviscous models were not supported by accurate measurements, the simple EoS (2) invokes non-physical behavior. First, the limit of compression, $\rho(p\to\infty)/\rho_0 = 1.353$, in equations (1) and (2), does not occur, although it may be argued that the glass transition imposes somewhat of a limit. Second, since this EoS fixes the compressibility independent of temperature and the longitudinal sound velocity at ambient pressure is approximately proportional to $\sqrt{K_0/\rho_0}$, the sound velocity is predicted to increase with temperature when ρ_0 must decrease. Of course, sound velocity in organic liquids decreases with temperature [12]. Third, if the simple EoS (2) is used to calculate the volume used in the Doolittle free-volume model [13] for viscosity, the inflection in the plot of log viscosity versus pressure never occurs.

The measurement of compressibility or the pressure dependence of density or volume for liquids is not as straightforward as might be expected [14] and requires some attention. The usual method employed in EHL laboratories is to use the pressure-generating piston-in-cylinder

device to directly measure the volume change as pressure is increased. While this apparatus is well suited to detect the small compressibility changes which accompany phase transitions, substantial errors will arise from measurements of the compressibility due to the inability to accurately account for vessel elastic deformation and from the contribution of the seal displacements [14]. The most widely accepted means of measuring compressibility of liquids to EHL pressures was introduced by Nobel laureate Bridgman [15]. This is the metal bellows volumometer or piezometer which has been improved over the years ([16] for example) and at least one commercial device is available to 200MPa.

The preferred isothermal EoS in physics-based fields is the Tait equation [17], actually a modification of the relation proposed by Tait, which for the relative volume reads:

$$\frac{V}{V_0} = 1 - \frac{1}{1+K_0'} \ln\left[1 + \frac{p}{K_0}\left(1+K_0'\right)\right] = \frac{\rho_0}{\rho} \qquad (3)$$

Here the parameters are defined as by Cook et al. [18] where K_0 is the bulk modulus at ambient pressure or $p = 0$ and K_0' is the pressure derivative of K at ambient pressure or $p = 0$. This EoS is often held to be the most accurate [19] of the simple relations, even for extrapolation to very high pressures [20]. For numerical EHL it has the advantage of providing an explicit formula for density as a function of pressure and tables of parameters are available for a vast number of liquids (see [21][22][23][24][25][26][27] for examples).

A modification of equation (3) will be necessary to incorporate temperature. The value of K_0' is often considered to be independent of temperature [26] and in some cases it has been assigned a universal constant $K_0' \equiv 10.2$ [25][27] although counter examples exist [17]. Here, K_0' is material dependent and temperature independent. Many expressions have been employed for the temperature dependence of K_0. Here the exponential form of Fakhreddine and Zoller [27] is used.

$$K_0 = K_{00} \exp\left(-\beta_K T\right) \qquad (4)$$

It is also required that V_0 vary with temperature and a linear dependence of density on temperature can be more accurate than a linear dependence of volume on temperature:

$$\begin{aligned} \frac{V_0}{V_R} = \frac{\rho_R}{\rho_0} &= \frac{1}{1 - a_\rho\left(T - T_R\right)} \quad \rightarrow \ \rho - T \text{ linear dependence} \\ \frac{V_0}{V_R} = \frac{\rho_R}{\rho_0} &= 1 + a_V\left(T - T_R\right) \quad \rightarrow \ V - T \text{ linear dependence} \end{aligned} \qquad (5)$$

The first attempt in numerical EHL simulation to use a more suitable EoS than equation (2) was by Venner and Bos [5] who employed a relation offered by Jacobson and Vinet [6].

$$p = 3K_0\left(\frac{V}{V_0}\right)^{\frac{-2}{3}}\left[1-\left(\frac{V}{V_0}\right)^{\frac{1}{3}}\right]\exp\left\{\frac{3}{2}\left(K_0'-1\right)\left[1-\left(\frac{V}{V_0}\right)^{\frac{1}{3}}\right]\right\} \qquad (6)$$

The Jacobson and Vinet equation (6) is unusual for an EHL EoS in solving for pressure as a function of the volume or density. Oddly, Jacobson and Vinet [6] found that a good representation of their experimental data was obtained by making K_0 in (6) independent of temperature. It should be noted that their experimental method would not be considered accurate according to the rules set forth by Hayward [14] since the elastic deformation of the pressure vessel must be accounted for in the measurement.

3. Thermal EHL model

In this section, the numerical model employed in this work is briefly reminded. The latter is based on the full-system finite element approach described in [28]. The generalized Reynolds, linear elasticity and load balance equations define the EHL part of the model. The Reynolds equation for a steady-state point contact between a ball and a flat plane lubricated with a generalized Newtonian lubricant under unidirectional surface velocities in the x-direction is given by Yang and Wen [29]:

$$\frac{\partial}{\partial x}\left[\left(\frac{\rho}{\eta}\right)_e h^3\frac{\partial p}{\partial x}\right]+\frac{\partial}{\partial y}\left[\left(\frac{\rho}{\eta}\right)_e h^3\frac{\partial p}{\partial y}\right]=12\frac{\partial}{\partial x}\left(\rho^* U_m h\right) \qquad (7)$$

Where:

$$U_m=\frac{u_p+u_s}{2} \qquad \left(\frac{\rho}{\eta}\right)_e=12\left(\frac{\eta_e\rho_e'}{\eta_e'}-\rho_e''\right)$$

$$\rho^*=\frac{\left[\rho_e'\eta_e\left(u_s-u_p\right)+\rho_e u_p\right]}{U_m} \qquad \rho_e=\frac{1}{h}\int_0^h\rho\,dz$$

$$\rho_e'=\frac{1}{h^2}\int_0^h\rho\int_0^z\frac{dz'}{\eta}dz \qquad \rho_e''=\frac{1}{h^3}\int_0^h\rho\int_0^z\frac{z'dz'}{\eta}dz$$

$$\frac{1}{\eta_e}=\frac{1}{h}\int_0^h\frac{dz}{\eta} \qquad \frac{1}{\eta_e'}=\frac{1}{h^2}\int_0^h\frac{z\,dz}{\eta}$$

Note that this equation accounts for the variations of both density and viscosity across the film thickness through the integral terms. In fact, the changes in density are due to temperature variations across the lubricant film whereas the changes in viscosity stem from both temperature and shear rate variations across the film. Moreover, both density and viscosity are allowed to vary with pressure and temperature throughout the lubricant film. Indices *p* and *s* correspond to

the plane and the sphere respectively and η is the generalized Newtonian viscosity. The film thickness *h* in equation (7) is replaced by:

$$h(x,y) = h_0 + \frac{x^2 + y^2}{2R} - \delta(x,y) \qquad (8)$$

Where *R* is the radius of the ball and *δ(x,y)* corresponds to the normal elastic deformation of the solid surfaces at every point *(x,y)* of the two-dimensional contact area Ω_c. It is obtained by solving the linear elasticity equations on a large *3D* solid body representing a half-space domain. To complete the EHL part, the load balance equation is used to monitor the value of the rigid body displacement h_0 and ensure that the correct external load *F* is applied to the contact. This equation reads:

$$\int_{\Omega_c} p \; d\Omega = F \qquad (9)$$

As for the thermal part, the temperature distribution in the two solid bodies and the lubricant film is obtained by solving the *3D* energy equation. For the solid parts *p* and *s* this equation reads:

$$\begin{cases} c_p \rho_p u_p \dfrac{\partial T}{\partial x} = k_p \left(\dfrac{\partial^2 T}{\partial x^2} + \dfrac{\partial^2 T}{\partial y^2} + \dfrac{\partial^2 T}{\partial z^2} \right) \\ c_s \rho_s u_s \dfrac{\partial T}{\partial x} = k_s \left(\dfrac{\partial^2 T}{\partial x^2} + \dfrac{\partial^2 T}{\partial y^2} + \dfrac{\partial^2 T}{\partial z^2} \right) \end{cases} \qquad (10)$$

The geometrical domains of solids *p* and *s* are taken as infinite layers with a finite thickness sufficiently large to have zero temperature gradient away from the contact area. As for the lubricant film, the energy equation is given by:

$$\rho c \left(u_f \frac{\partial T}{\partial x} + v_f \frac{\partial T}{\partial y} \right) = k \frac{\partial^2 T}{\partial z^2} - \frac{T}{\rho} \frac{\partial \rho}{\partial T} \left(u_f \frac{\partial p}{\partial x} + v_f \frac{\partial p}{\partial y} \right) + \eta \left[\left(\frac{\partial u_f}{\partial z} \right)^2 + \left(\frac{\partial v_f}{\partial z} \right)^2 \right] \qquad (11)$$

Where the lubricant velocity field components u_f and v_f in the *x* and *y* directions respectively are given by:

$$\begin{aligned} u_f &= u_p + \frac{\partial p}{\partial x} \left[\int_0^z \frac{z' dz'}{\eta} - \frac{\eta_e}{\eta_e'} h \int_0^z \frac{dz'}{\eta} \right] + \frac{\eta_e (u_s - u_p)}{h} \int_0^z \frac{dz'}{\eta} \\ v_f &= \frac{\partial p}{\partial y} \left[\int_0^z \frac{z' dz'}{\eta} - \frac{\eta_e}{\eta_e'} h \int_0^z \frac{dz'}{\eta} \right] \end{aligned} \qquad (12)$$

Equations (7-12) completely define the thermal EHL problem. These equations are solved using the usual EHL boundary conditions. That is, for the generalized Reynolds equation zero pressure is assumed on the boundary of the contact area Ω_c and the free boundary problem arising at the exit of the contact is handled by applying the penalty method [30]. As for the linear elasticity part, the pressure distribution obtained from Reynolds equation is used as a normal pressure load boundary condition on the contact surface Ω_c. Finally, for the thermal part, an ambient temperature T_0 boundary condition is applied at the inlet of the solid bodies and the lubricant film.

4. Numerical procedure

All equations defined in the previous section are discretized using a finite element approximation and solved in dimensionless form [28]. Non-structured meshing is used throughout the different parts of the problem. For the hydrodynamic part (generalized Reynolds equation), fifth order Lagrange triangular elements (2D) are employed whereas for the elastic part Lagrange second order tetrahedral elements (3D) are used. Using higher order elements for the hydrodynamic problem, as an alternative to refining the mesh, allows having a good precision for its solution without inducing any unnecessary increase in the number of degrees of freedom in the three-dimensional elastic problem. For the thermal part, Lagrange second order tetrahedral elements are also employed. The meshing of all geometric components is tailored towards the nature of the EHL problem. That is, the mesh is always finer in the central area of the contact (mesh diameter ~ 0.05) where additional precision is required owing to the sharper solution gradients that are encountered. For more details regarding the geometry and its meshing, the reader is referred to [28].

The global numerical procedure consists in starting with an initial guess for pressure, film thickness and temperature. The generalized Reynolds, linear elasticity and load balance equations are solved simultaneously using a damped Newton [31] resolution. The resulting pressure and film thickness distributions are then used to solve the thermal problem defined by equations (10-12) which are also solved simultaneously. An iterative procedure is thus established between the respective solutions of the EHL and thermal problems. This iterative procedure is repeated until the pressure and temperature solutions are converged, that is until the maximum absolute difference between the pressure solutions and the maximum relative difference between the temperature solutions at two consecutive resolutions falls below 10^{-3}. Note that for highly loaded contacts, special stabilized finite element formulations are needed for the solution of the generalized Reynolds equation. Similar formulations are also needed for the solution of the energy equations in a convection-dominated regime. For more details about the convergence criteria, the definition of the penalty term for the treatment of the free boundary problem and the numerical precision of this solution scheme the reader is referred to [28].

5. Properties of simulated liquids

Numerical experiments are performed for two liquids possessing different compressibility characteristics which were obtained from measurements, known to be accurate, on real liquid lubricants. For the sake of isolating compressibility effects, all other liquid properties are kept unchanged (viscosity, thermal conductivity, heat capacity…). These are summarized in Table 1 along with the properties of the solids (both the sphere and the plane are assumed to be made out of steel). The reference temperature T_R=25°C for both considered lubricants. Density and viscosity parameters are provided in the following sections.

	Solids	Lubricants
Thermal Conductivity (W/m.K)	46	0.15
Heat Capacity (J/kg.K)	470	1500
Density (kg/m^3)	7850	900 (at T_R)
Young's Modulus (GPa)	210	-
Poisson's Coefficient	0.3	-
Equivalent Radius (mm)	15	-

Table 1: Lubricants and solids material properties

5.1 Compressibility

Surprisingly, many accurate experimental measurements of viscosity and density for lubricating oils to 1 GPa and 218°C have been available throughout the development of the EHL field as reported in the 1953 report of the ASME Research Committee on Lubrication [28]. These results were generated at the Harvard University laboratory of Nobel laureate, P.W. Bridgman. For the numerical work to follow, two model liquids were chosen from the ASME report; the most compressible, a silicone oil (ASME 55), and the least compressible, a heavy naphthenic mineral oil (ASME 38). The Tait EoS has been fitted to these data as shown in Figure 1 with the parameters listed in Table 2. The *V*-*T* linear dependence relationship has been used to specify the temperature dependence at ambient pressure because the use of a ρ-*T* linear dependence relationship which is actually more precise at ambient pressure results in the crossing of isotherms for the silicone oil at *T*=473K and *p*=1.4 GPa. Some accuracy at ambient pressure has therefore been sacrificed to avoid non-physical response at elevated pressure.

	ASME sample 38	ASME sample 55
K_0'	9.650	9.735
K_{00} (GPa)	5.792	4.196
β_K (K^{-1})	0.003791	0.005318
a_V (K^{-1})	0.000679	0.000984

Table 2: Tait parameters for the model liquids

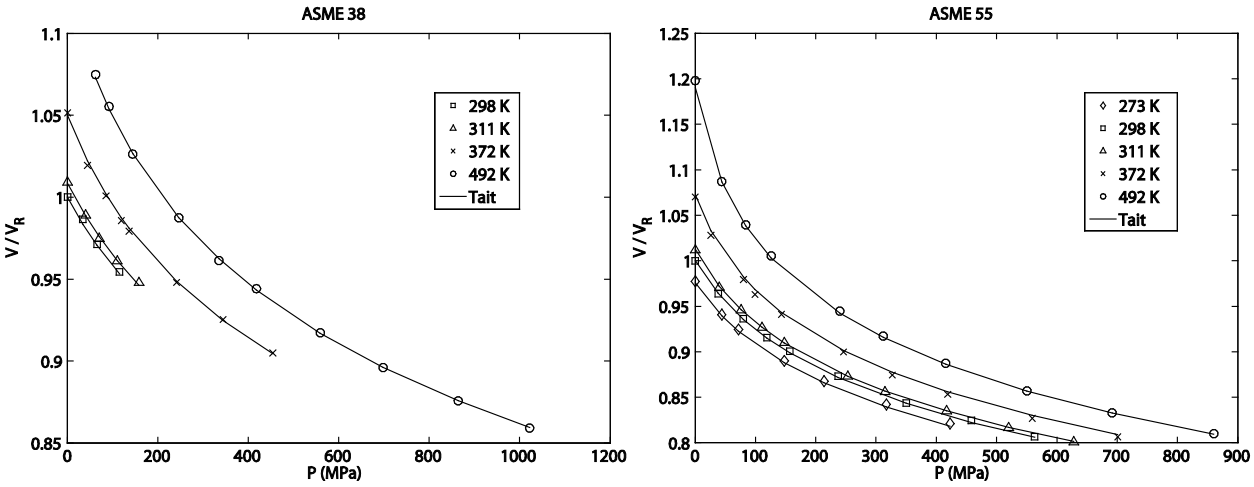

Figure 1: The ASME relative volumes of the naphthenic mineral oil (ASME 38) and the silicone oil (ASME 55) and their fit to theTait EoS

The Jacobson and Vinet equation (6) provides an excellent fit to the data for the silicone oil only when K_0 is a function of temperature as in equation (4). The parameters are $K_0' = 11.308$, $K_{00} = 4.946$ GPa , $\beta_K = 0.006046\ \mathrm{K}^{-1}$ and $a_V = 0.000897\mathrm{K}^{-1}$.

5.2 Viscosity

The most precise temperature-pressure correlations for the thermophysical properties of liquids are obtained from thermodynamic scaling [33] which represents the property as a function of temperature and volume (or density). This representation is, however, not possible here because the intent is to compare only the effect of compressibility with the remaining property relations being the same. For this purpose, the temperature and pressure dependence of the low shear viscosity, $\mu(T, p)$, of a viscosity reference liquid, diisodecyl phthalate [34], and the shear dependent viscosity, $\eta(\mu, \tau)$, of a similar diester, di(2-ethylhexyl) phthalate [35], will be used in the numerical experiments.

A correlation of the low shear viscosity of diisodecyl phthalate which does not require an EoS has been published [36]. The Vogel, Tammann and Fulcher equation [37] with pressure dependent divergence temperature is:

$$\mu = \mu_\infty \exp\left[\frac{D_F T_\infty(p)}{T - T_\infty(p)}\right] \qquad \text{with} \quad T_\infty = T_0 - \frac{T_0'^2}{T_0''}\ln\left(1 - \frac{T_0''}{T_0'}p\right) \tag{13}$$

The parameters which describe the diester are $\mu_\infty = 3.655\times10^{-6}$ Pa·s, $D_F = 16.30$, $T_0 = 114.4$ K, $T_0' = 146.0$ K/GPa and $T_0'' = -331.1$ K/GPa^2.

The shear dependence of viscosity of di(2-ethylhexyl) phthalate is represented by a modified Carreau equation [36] written in terms of shear stress, τ.

$$\eta = \mu\left[1+\left(\frac{\tau}{G}\right)^2\right]^{\frac{1-\frac{1}{n}}{2}} \qquad (14)$$

The parameters are, from [35], $n = 0.41$ and $G = 6$ MPa.

6. Results

In this section, numerical tests are carried out to study compressibility effects on lubricant film thickness under thermal EHL conditions. As mentioned earlier, in order to isolate compressibility effects, all physical parameters (lubricant viscosity, solid material properties, etc.) are kept constant throughout the tests except for lubricant density. Three different densities are considered: ASME 38 and ASME 55 according to the Tait EoS and the Dowson & Higginson density. The latter being material independent, corresponding film thicknesses are compared to those obtained using the first two. This allows a quantification of the error involved in using the Dowson & Higginson relationship in modeling lubricant density. A wide variety of operating conditions is considered with different loads *F*, inlet temperatures T_0, mean entrainment speeds U_m and slide-to-roll ratios *SRR* defined as:

$$SRR = \frac{u_s - u_p}{U_m} \qquad (15)$$

The results of all numerical tests are summarized in Tables 3 and 4. Table 3 provides the pure-rolling (*SRR*=0) test results for various loads, mean entrainment speeds and inlet temperatures whereas Table 4 provides rolling-sliding results. $|\Delta H_c|/H_c$ corresponds to the relative error induced by using the Dowson & Higginson relationship on the dimensionless central film thickness H_c defined as:

$$\frac{|\Delta H_c|}{H_c} = \frac{\left|H_c(Tait) - H_c(D\&H)\right|}{H_c(Tait)} \qquad (16)$$

Only the effect on central film thickness is reported in this section as it is observed that the minimum film thickness is barely affected by compressibility as noted by Venner and Bos [5]. Several conclusions may be drawn from the results of Tables 3 and 4.

First, from Table 3 it can be noted that the relative error induced by using the Dowson & Higginson relationship continuously increases with increasing load. This is not surprising, as for both model liquids, density difference between the Tait EoS and Dowson & Higginson relationship continuously increases with pressure as can be seen in Figure 2. Remember that Venner and Bos [5] observed that central film thickness decreases linearly with the increase in compression in isothermal EHL contacts. It is noteworthy to mention that this observation still holds here under thermal conditions. The error increase with load is observed for both ASME 38 and 55 except for the low temperature cases (30^{o}C) of the former where the error is minimal for the 90N load (p_h≈1GPa) and then increases as the load departs from that value. In fact, by observing Figure 2 (left) closely, one can note that for 30^{o}C the density lines of Tait and Dowson & Higginson cross at ≈1GPa and deviate as the pressure departs from that value. This explains the minimum value of error obtained for the 90N case with an inlet temperature of 30^{o}C. Figure 3 shows a comparison of the dimensionless film thickness profiles along the central line of the contact in the x-direction for both ASME 38 and 55 (Tait) with respect to those obtained using the Dowson & Higginson relationship for an inlet temperature of 30^{o}C. These clearly highlight the error trends discussed so far. Note that the use of the Dowson & Higginson relationship leads to an overprediction of the central film thickness except for the low load case of ASME 38. This is because at 30^{o}C, the Dowson & Higginson relationship predicts a higher density for ASME 38 than the Tait EoS up to ≈ 1 GPa (see Figure 2). Also note, that the errors are always more important for ASME 55 compared to ASME 38 which is not surprising as the density deviations for the latter with respect to the Dowson & Higginson relationship are smaller as can be seen in Figure 2.

T_0(°C)	F(N)	U_m(m/s)	$\lvert\Delta H_c\rvert/H_c$ (%)	
			ASME 38	ASME 55
30	10 ($p_h \approx 0.5$GPa)	0.1	1.07	3.49
		0.2	1.04	3.43
		0.5	0.99	3.33
		1.0	1.38	2.74
		2.0	0.86	3.02
	90 ($p_h \approx 1.0$GPa)	0.1	0.08	6.14
		0.2	0.10	6.15
		0.5	0.14	6.11
		1.0	0.17	6.09
		2.0	0.33	5.57
	300 ($p_h \approx 1.5$GPa)	0.1	1.74	8.51
		0.2	1.77	8.58
		0.5	1.82	8.63
		1.0	1.84	8.62
		2.0	1.36	8.14
	700 ($p_h \approx 2.0$GPa)	0.1	3.51	10.78
		0.2	3.48	10.77
		0.5	3.51	10.91
		1.0	3.54	10.95
		2.0	3.07	10.45
100	10 ($p_h \approx 0.5$GPa)	0.5	0.09	4.63
		1.0	0.08	4.48
		2.0	0.07	4.35
	90 ($p_h \approx 1.0$GPa)	1.0	1.39	7.53
		2.0	1.40	7.45
	300 ($p_h \approx 1.5$GPa)	1.0	3.23	10.26
		2.0	3.25	10.13
		10.0	2.75	9.46
	700 ($p_h \approx 2.0$GPa)	2.0	5.08	12.61
		10.0	4.55	11.84
200	10 ($p_h \approx 0.5$GPa)	2.0	1.02	5.93
		5.0	0.96	5.56
	90 ($p_h \approx 1.0$GPa)	5.0	2.80	9.18
	300 ($p_h \approx 1.5$GPa)	10.0	5.05	12.20
	700 ($p_h \approx 2.0$GPa)	10.0	7.05	15.33

Table 3: ASME 38 and 55 pure-rolling numerical tests results for various load, mean entrainment speed and inlet temperature conditions

Second, it can be noted from Table 3 that the mean entrainment speed U_m has very little influence on the error induced by the use of the Dowson & Higginson relationship and the error remains almost unchanged regardless of speed. This is because for a given load, the mean entrainment speed has little effect on the overall magnitude of the pressure distribution in the contact and thus on lubricant density.

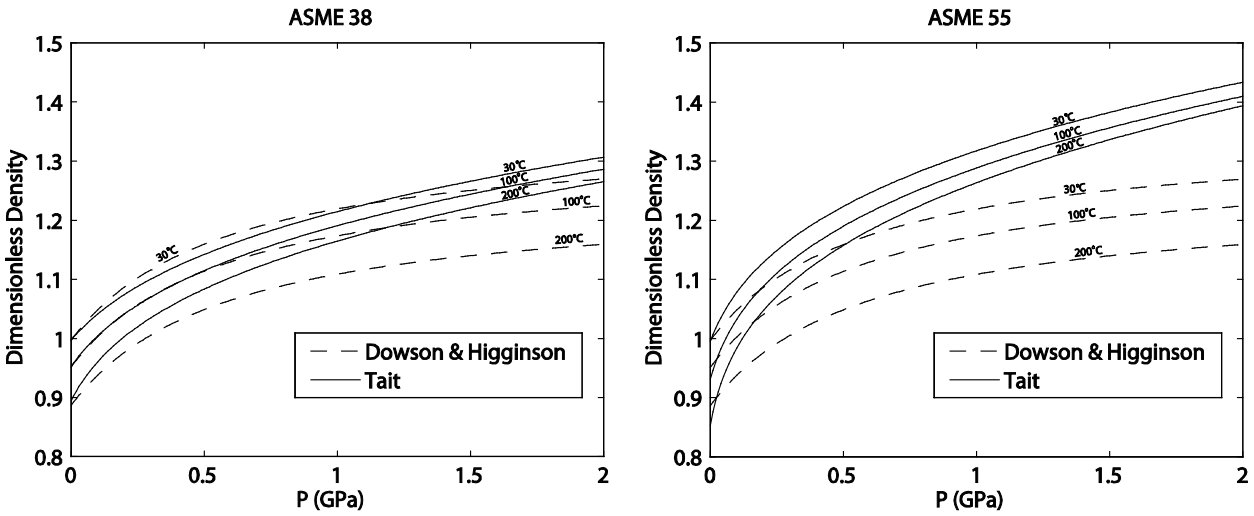

Figure 2: Comparison of the Tait EoS and Dowson & Higginson relationship for dimensionless density of ASME 38(left) and ASME 55 (right) lubricants as a function of pressure

Finally, from Table 3 it can be observed that error increases with inlet temperature T_0 for both ASME 38 and 55. This is because the deviation of the Tait EoS from the Dowson & Higginson relationship continuously increases with temperature as can be seen in Figure 2. This is true except for the low load cases of ASME 38 where the deviation is almost nill for T0=100°C and smaller than for T0=30°C. This explains the minimum errors obtained for T0=100°C for the low load case (F=10N). To conclude, it can be said that errors increase with temperature in general (not only inlet temperature) as highlighted by the results of Table 4.

T_0(°C)	F(N)	U_m(m/s)	SRR	$\lvert\Delta H_c\rvert/H_c$ (%)	ΔT_{max} (°C)
30	90 ($p_h \approx$ 1.0GPa)	1.0	0.0	6.09	0.22
			0.5	6.88	44.68
	300 ($p_h \approx$ 1.5GPa)	2.0	0.0	8.14	1.81
			0.5	10.65	91.49
100	90 ($p_h \approx$ 1.0GPa)	1.0	0.0	7.53	0.03
			0.5	7.75	9.44
	300 ($p_h \approx$ 1.5GPa)	2.0	0.0	10.13	0.09
			0.5	11.31	36.76

Table 4: ASME 55 rolling-sliding numerical test results for various load, mean entrainment speed and inlet temperature conditions

Table 4 presents the results of the numerical tests for ASME 55 under rolling-sliding conditions. It is clear that the error induced by employing the Dowson & Higginson relationship for density not only increases with the inlet temperature T_0 but also with temperature in general. This is highlighted by the larger variations in error between the pure-rolling cases (SRR=0) and the rolling-sliding cases (SRR=0.5) observed for the lower inlet temperature case (T_0=30°C). These can be associated to the higher increase in temperature as suggested by the values of the maximum temperature increase ΔT_{max} within the lubricant film reported in Table 4. These greater temperature rises are due to the higher viscosities obtained at lower surrounding

temperature T_0 leading to an increased thermal dissipation by shear, all other operating conditions being unchanged.

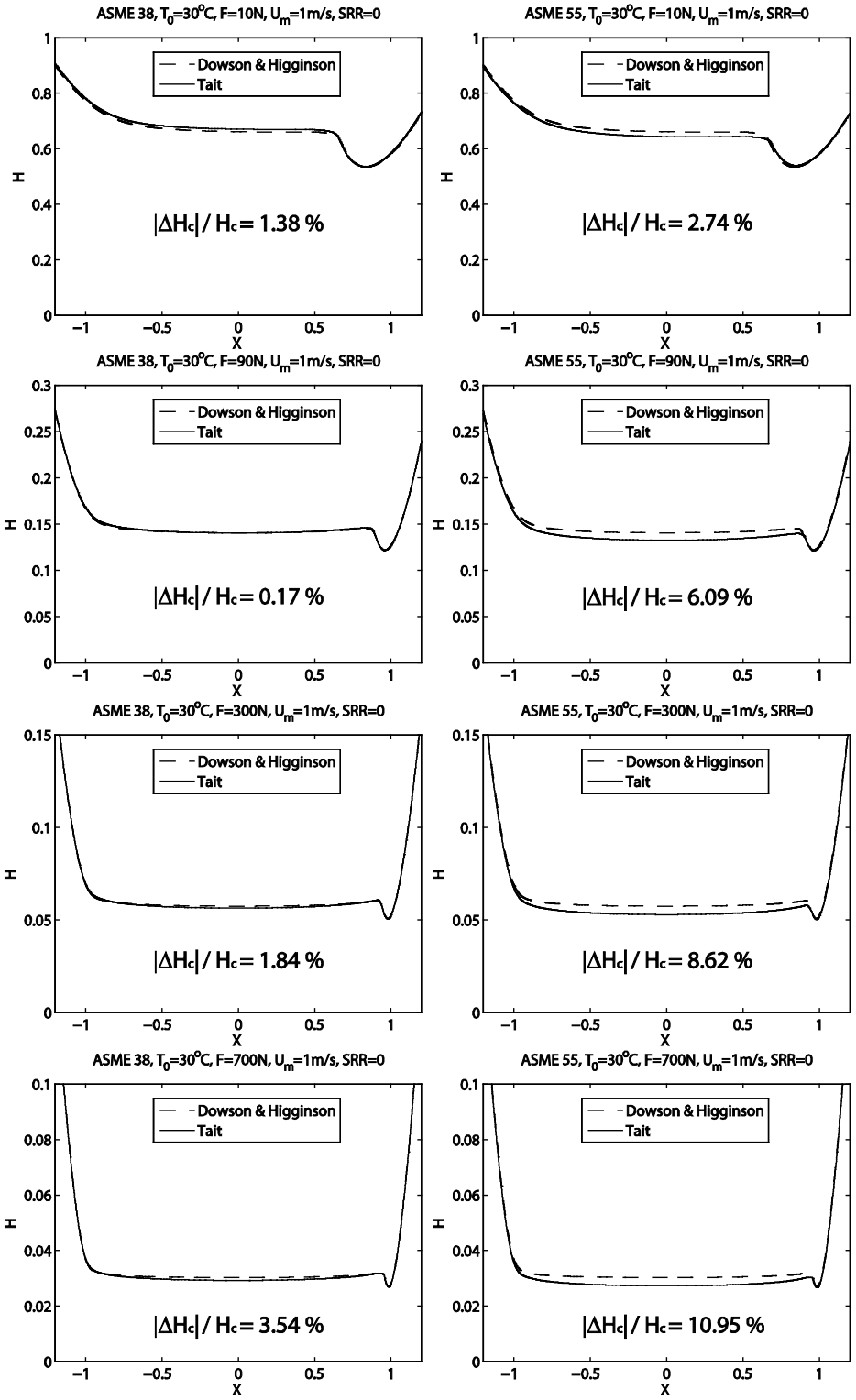

Figure 3: Comparison of dimensionless film thickness profiles along the central line of the contact in the x-direction obtained under pure-rolling conditions using the Tait EoS for both ASME 38 (left) and ASME 55(right) with respect to those obtained using the Dowson & Higginson relationship (T_0=30°C)

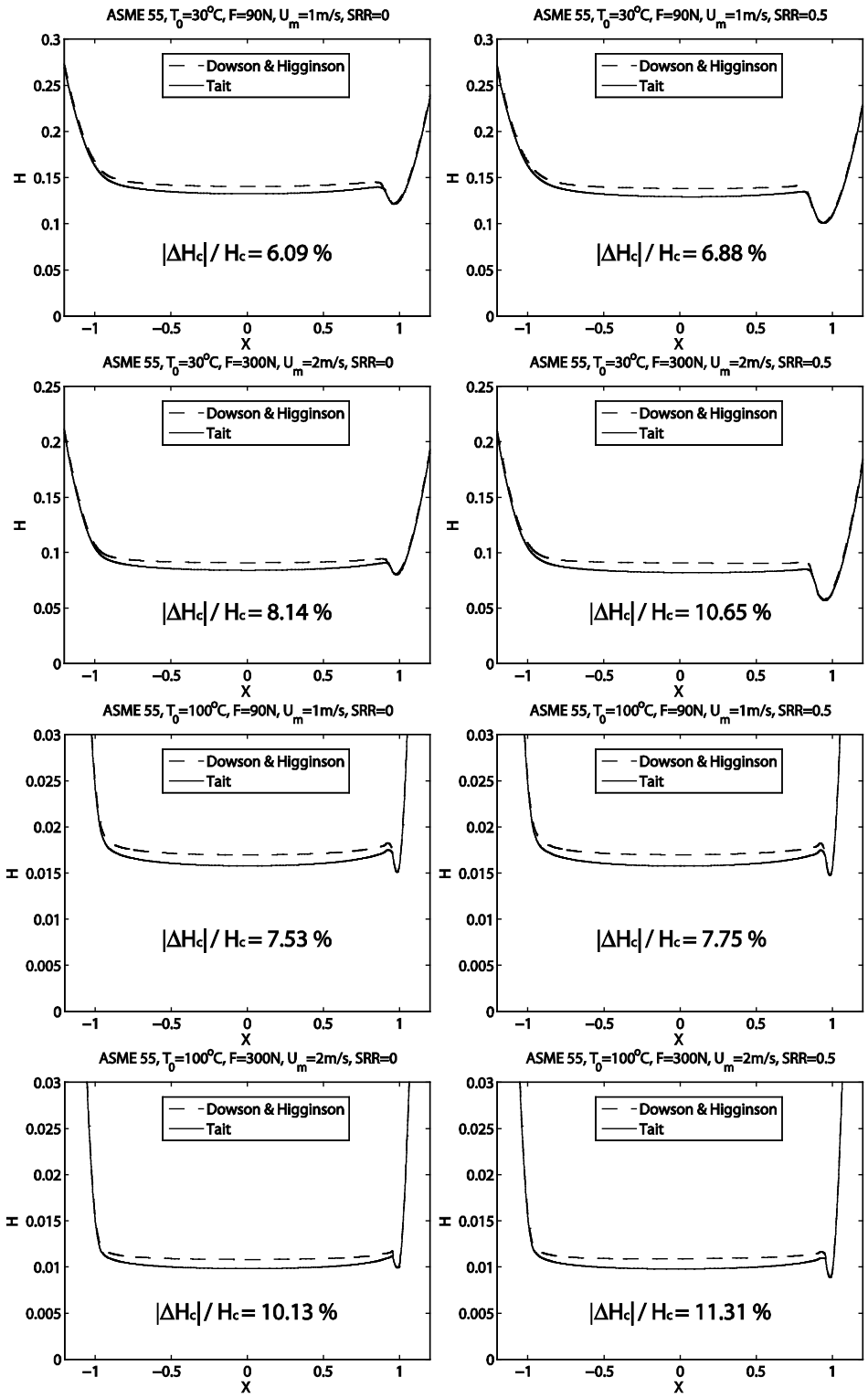

Figure 4: Comparison of dimensionless film thickness profiles along the central line of the contact in the x-direction obtained using the Tait EoS for ASME 55 with respect to those obtained using the Dowson & Higginson relationship for *SRR*=0 (left) and *SRR*=0.5 (right) with T_0=30°C (top figures) and T_0=100°C (bottom figures)

Figure 4 shows comparison plots of the dimensionless film thickness profiles along the central line of the contact in the x-direction for ASME 55 (Tait) with respect to those obtained using the Dowson & Higginson relationship for slide-to-roll ratios *SRR*=0 (left) and *SRR*=0.5 (right) for the cases reported in Table 4. These plots reveal the error trends discussed above. Also note the well-known change in the horseshoe shape of the film thickness profile due to thermal effects. In fact, when the *SRR* is increased, the minimum film thickness on the central line of the contact in the *x*-direction decreases and approaches the global minimum film thickness and the film thickness constriction gains in width. Therefore, the horseshoe shape at the outlet of the contact, which originally has large ends and a narrow central region, gains in width on its central part and starts having an almost constant width. This feature was highlighted for instance in the numerical tests of [9] or the experimental results of [38].

7. Discussion

The Venner and Bos rule [5] for the correction of the central film thickness from an incompressible solution can be expressed as:

$$h_c = h_{c,i} \frac{V\left(p = p_h\right)}{V\left(p = 0\right)} \qquad (17)$$

Where $h_{c,i}$ is the central film thickness that would be obtained if the lubricant was assumed to be incompressible. This equation can be easily generalized to:

$$h_c\big|_{EoS_1} = h_c\big|_{EoS_2} \frac{V\big|_{EoS_1}\left(p = p_h\right)}{V\big|_{EoS_2}\left(p = p_h\right)} \qquad (18)$$

so that different compressibilities may be compared. In fact, here it is found that this rule may be extended to the thermal case by substituting in (17) and (18) V at the inlet temperature and $p = 0$ for $V\left(p = 0\right)$ and by substituting V at the central film temperature and $p = p_h$ for $V\left(p = p_h\right)$.

There are some consequences of the widespread use of a simple EoS such as equation (2). Most values of pressure-viscosity coefficient published recently have been the effective pressure-viscosity coefficient obtained by forcing agreement of a classical film thickness formula with a measurement of central film thickness in a circular contact as, for example, in [39]. When there are viscosities measured under high pressure for comparison, these effective pressure-viscosity coefficients are often much smaller than the coefficients derived from a real viscosity measurement. The primary reason is the neglect of the shear dependence of viscosity [40]. However, the assumed compressibility may play a significant role in the discrepancies. If all other effects are precisely as were assumed for the film thickness formula and if $h_c \propto \alpha^{*0.53}$ as it is for the classical Hamrock & Dowson film thickness formula [3]:

$$\alpha \propto h_c^{1.89} \qquad (19)$$

However, if the compressibility is not the same as was assumed for the formula, then from the Venner and Bos rule (18), the proper relation for a pressure-viscosity coefficient derived from film thickness measurements would be:

$$\alpha \propto h_c^{1.89} \left[V\left(p = p_h\right) / V\left(p = 0\right) \right]^{-1.89} \qquad (20)$$

Unfortunately, the real compressibilities of the liquids for which the effective coefficients have been reported are seldom known. The possible errors in effective coefficients may be investigated from the examples in this paper. In Figure 5, the measured pressure-viscosity coefficient α^* is plotted versus temperature for diisodecyl phthalate as the solid curve. If all other effects are precisely accounted for in a film thickness formula which employed the Dowson & Higginson relationship, then the effective coefficient is related to the real pressure-viscosity coefficient α^* by:

$$\alpha_{eff} = \alpha^* \left[\frac{V\left(p = p_h\right)}{V\big|_{Dow\&Hig}\left(p = p_h\right)} \right]^{1.89} \qquad (21)$$

This effective coefficient has been plotted in Figure 5 for the compressibility of ASME 55 as the dotted curve and that of ASME 38 as the dashed curve. In other words, the dashed and dotted curves represent the values of pressure-viscosity coefficient which would be reported from a film thickness measurement using the established technique (equation (19)) while the solid curve is the coefficient which would be obtained from a viscometer. The discrepancies are temperature dependent and may be quite large, almost 30% for the highest temperature and pressure.

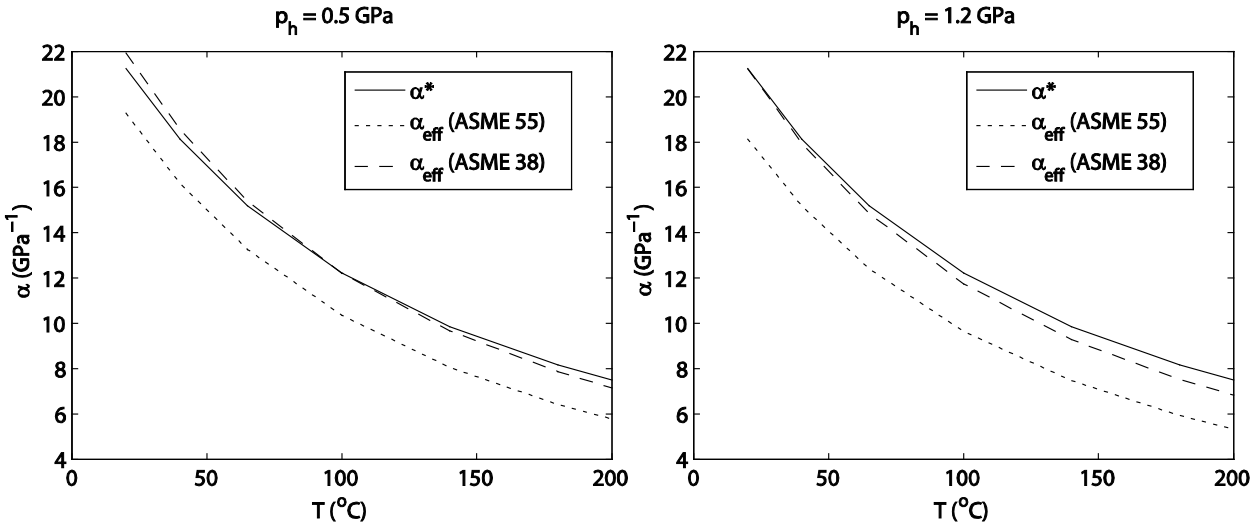

Figure 5: Comparison of effective pressure-viscosity coefficients using assumed compressibilities with the directly measured coefficient.

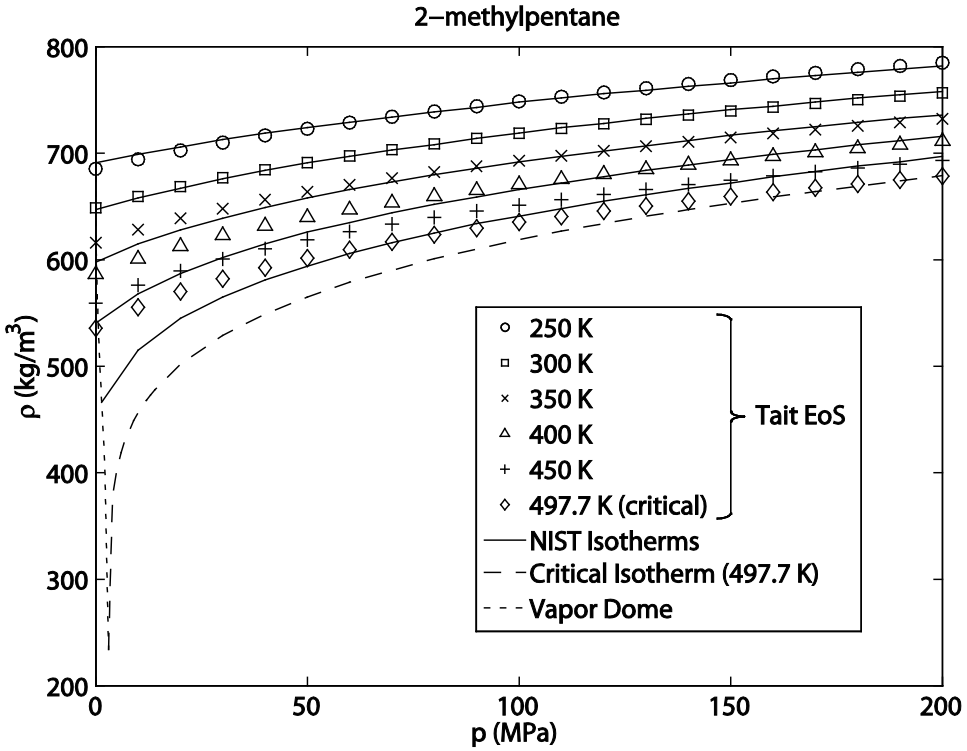

Figure 6: Comparison of real (certified by NIST) density variations of 2-methylpentane against pressure and temperature with those predicted by the Tait EoS

It is necessary to warn against the overenthusiastic use of universal equations of state, even those based on Tait (3). For example, process liquids such as fuels or even refrigerants have been investigated as possible ultra-low-viscosity EHL lubricants. These liquids may be used under conditions of temperature and pressure sufficiently close to the critical point to display compressibility very different from that of the compressed liquids which are ordinarily addressed in EHL. The difficulty imposed by very low molecular mass liquids is illustrated in Figure 6 where the density of 2-methyl pentane is plotted against pressure for various isotherms. The critical isotherm must be vertical on this plot at the critical density. This requirement is, of course, not met by any EoS employed in EHL. The curves plotted in Figure 6 are the densities certified by NIST [41]. The vapor dome is shown for reference. The points represent the Tait EoS (3) with $K_0' = 10.29$, $K_{00} = 2.168$ GPa, $\beta_K = 0.004492\ \mathrm{K}^{-1}$ and $a_V = 0.001127\mathrm{K}^{-1}$. The fit at critical temperature, 225°C, is poor below 150 MPa and the fit at ambient pressure is poor above 27°C.

8. Conclusion

This paper highlights the importance of using realistic modeling of lubricant compressibility for an accurate numerical prediction of central film thicknesses in thermal EHL circular contacts. Lubricants have density-pressure-temperature dependencies that do not necessarily follow the commonly used Dowson & Higginson relationship especially at high pressures and temperatures. Numerical film thickness predictions using the classical Dowson and Higginson relationship are

compared to those obtained using a more realistic compressibility model, all other parameters kept unchanged. In order to achieve as realistic as possible predictions, the authors considered two model liquids from the 1953 report of the ASME Research Committee on Lubrication, the most and the least compressible. The compressibility of these liquids is modeled using the Tait equation of state (EoS) while all other transport properties are kept unchanged for the sake of isolating compressibility effects. In addition, the same typical generalized-Newtonian behavior is assumed for both model liquids. While the errors in predicting minimum film thickness are negligible, the central film thickness errors are pronounced. In most cases, the Dowson & Higginson relationship underpredicts lubricant density leading to an overprediction of central film thicknesses. The Venner and Bos rule is confirmed; the central film thickness varies in proportion to the volume compression. It is found that the relative errors on central film thicknesses increase with load and temperature and are very little affected by mean entrainment speed. Compressibility can be a significant source of error in film-derived measurements of pressure-viscosity coefficients especially at high temperature. The thermodynamic scaling which provides an accurate and consistent framework for the correlation of the thermophysical properties of liquids with temperature and pressure requires an accurate equation of state.

Acknowledgments

The first author wishes to thank the Council for International Exchange of Scholars (CIES) and the Fullbright commission for funding his visiting scholar program at the Georgia Institute of Technology. Bair was supported by the Center for Compact and Efficient Fluid Power, a National Science Foundation Engineering Research Center funded under cooperative agreement number EEC-0540834.

Nomenclature

a_V : thermal expansivity defined for volume linear with temperature, K^{-1}
a_ρ : thermal expansivity defined for density linear with temperature, K^{-1}
c : lubricant thermal heat capacity, J/kg.K
c_p : thermal heat capacity of plane's material, J/kg.K
c_s : thermal heat capacity of sphere's material, J/kg.K
D_F : fragility parameter in the VTF equation
E' : composite Young's modulus, Pa
F : external applied load, N
G : shear modulus, liquid critical shear stress, Pa
h : film thickness, m
H : dimensionless film thickness
h_c : central film thickness, m
H_c : dimensionless central film thickness
h_m : minimum film thickness, m

H_m : dimensionless minimum film thickness

h_0 : rigid body separation, m

k : lubricant thermal conductivity, W/m.K

k_p : thermal conductivity of plane's material, W/m.K

k_s : thermal conductivity of sphere's material, W/m.K

K_0 : isothermal bulk modulus at p = 0, Pa

K_0' : pressure rate of change of isothermal bulk modulus at p = 0

K_{00} : K_0 at zero absolute temperature, Pa

n : power-law exponent

p : pressure, Pa

SRR : slide-to-roll ratio

T : temperature, K

T_R : reference temperature, K

T_0 : ambient pressure value of T_∞, K

T_0' : ambient pressure value of dT_∞ / dp, K/Pa

T_0'' : ambient pressure value of d^2T_∞ / dp^2, K/Pa^2

T_∞ : divergence temperature, K

u_p : plane surface velocity, m/s

u_s : sphere surface velocity, m/s

u_f : lubricant velocity component in x-direction, m/s

v_f : lubricant velocity component in y-direction, m/s

U_m : mean entrainment speed, m/s

V : volume at T and p, m^3

V_R : volume at reference state, T_R, p = 0, m^3

V_0 : volume at p = 0, m^3

x,y,z : space coordinates

α_0 : initial pressure-viscosity coefficient, Pa^{-1}

α^* : reciprocal asymptotic isoviscous pressure coefficient ($=1/p_{ai}$), Pa^{-1}

α_{film} : general film-forming pressure-viscosity coefficient, Pa^{-1}

β_K : temperature coefficient of K_0, C^{-1}

ΔT_{max}: maximum temperature elevation within lubricant film (^{o}C)

$\dot{\gamma}$: shear rate, s^{-1}

η : rate-dependent shear viscosity, Pa$\cdot$s

μ : limiting low-shear viscosity and Newtonian viscosity, Pa$\cdot$s

μ_0 : low-shear viscosity at p=0, Pa·s

Ω_c : Contact area geometric domain

ρ : lubricant mass density, kg/m^3

ρ_0 : lubricant mass density, at p = 0, kg/m^3

ρ_p : mass density of plane's material, kg/m^3

ρ_s : mass density of sphere's material, kg/m^3

τ : shear stress, Pa

References

[1] Dowson, D. and Higginson, G.R., 1959, "A Numerical Solution of the Elastohydrodynamic Problem," Proc. Inst. Mech. Eng., Part C: J. Mech. Eng. Sci., **1** (1), pp. 6-15.

[2] Hamrock, B.J. and Dowson, D., 1976, "Isothermal Elastohydrodynamic Lubrication of Contacts, Part I - Theoretical Formulation," ASME J. Lubr. Techn., **98** (2), pp. 223-229.

[3] Hamrock, B.J. and Dowson, D., 1977, "Isothermal Elastohydrodynamic Lubrication of Point Contacts, Part III – Fully Flooded Results," ASME J. Lubr. Techn., **99** (2), pp. 264-276.

[4] Kweh, C. C., Evan, H. P. and Snidle, R.W., 1989, "Elastohydrodynamic Lubrication of Heavily Loaded Circular Contacts," Proc. Inst. Mech. Eng., Part C: J. Mech. Eng. Sci., **203**, pp. 133-148.

[5] Venner, C. H. and Bos, J., 1994, "Effects of Lubricant Compressibility on the Film Thickness in EHL Line and Circular Contacts," Wear, **173**, pp. 151-165.

[6] Jacobson, B. and Vinet, P., 1987, "A Model for the Influence of Pressure on the Bulk Modulus and the Influence of Temperature on the Solidification Pressure for Liquid Lubricants," ASME J. Tribol., **109** (4), pp. 709-714.

[7] Dowson, D., Higginson, G.R. and Whitaker, A.V., 1962, "Elasto-Hydrodynamic Lubrication: A Survey of Isothermal Solutions," Proc. Inst. Mech. Eng., Part C: J. Mech. Eng. Sci., **4** (2), pp. 121-126.

[8] López, E.R., Pensado, A.S., Fernández, J. and Harris, K.R., 2012, "On the density scaling of pVT data and transport properties for molecular and ionic liquids," J. Chem. Phys. **136**, 214502.

[9] Habchi, W., Eyheramendy, D., Bair, S., Vergne, P. and Morales-Espejel G., 2008, "Thermal Elastohydrodynamic Lubrication of Point Contacts Using a Newtonian / Generalized Newtonian Lubricant," Tribol. Lett., **30** (1), pp. 41-52.

[10] Habchi, W., Vergne, P., Bair, S., Andersson, O., Eyheramendy, D. and Morales-Espejel, G.E., 2010, "Influence of Pressure and Temperature Dependence of Thermal Properties of a Lubricant on the Behaviour of Circular TEHD Contacts," Tribol. Int., **43**, pp. 1842-1850.

[11] Kaneta, M. and Yang, P., 2010, “Effects of the Thermal Conductivity of Contact Materials on Elastohydrodynamic Lubrication Characteristics,” Proc. Inst. Mech. Eng., Part C: J. Mech. Eng. Sci., **224** (12), pp. 2577-2587.

[12] Crocker, M.J., 1998, “Handbook of Acoustics,” New York: Wiley, pp. 69-71.

[13] Doolittle, A.K., 1951, “Studies in Newtonian Flow. II. The Dependence of the Viscosity of Liquids on Free-Space," J. Appl. Phys., **22** (12), pp. 1471 - 1475.

[14] Hayward, A.T.J., 1971, “How to Measure the Isothermal Compressibility of Liquids Accurately,” J. Phys. D: Appl. Phys., **4** (7), pp. 938-950.

[15] Bridgman, P.W., 1931, “The Physics of High Pressure,” New York: Dover, pp. 126-127.

[16] Back, P.J., Easteal, A.J., Hurle, R.L. and Woolf, L.A., 1982, “High-Precision Measurements with a Bellows Volumometer,” *J. Phys. E: Sci. Instr.*, **15** (3), pp.360-363.

[17] Dymond, J. H. and Malhotra, R., 1988, “The Tait Equation: 100 Years On,” Int. J. Thermophys., **9** (6), pp. 941-951.

[18] Cook, R.L., King, H.E., Herbst, C.A. and Herschbach, D.R., 1994, “Pressure and Temperature Dependent Viscosity of Two Glass Forming Liquids: Glycerol and Dibutyl Phthalate”, J. Chem. Phys., **100** (7), pp. 5178-5189.

[19] Hirschfelder, J.O., Curtiss, C.F. and Bird, R.B., 1954, “Molecular Theory of Gases and Liquids,” Wiley, New York, p.261.

[20] Millat, J., Dymond, J.H. and de Castro, C.A.N., 1996, “Transport Properties of Fluids Their Correlation, Prediction and Estimation,” IUPAC, Cambridge, p.172.

[21] Tanaka, Y., Nojiri, N., Ohta, K., Kubota, H. and Makita, T., 1989, “Density and Viscosity of Linear Perfluoropolyethers under High Pressures,” Int. J. Thermophys., **10** (4), pp.857-870.

[22] Cibulka, I. and Takagi, T., 1999, “P−ρ−T Data of Liquids: Summarization and Evaluation. 5. Aromatic Hydrocarbons,” J. Chem. and Eng. Data, **44** (3), pp. 411-429.

[23] Cibulka, I., Hnědkovský, L. and Takagi, T., 1997, “P-ρ-T Data of Liquids: Summarization and Evaluation. 4. Higher 1-Alkanols (C11, C12, C14, C16), Secondary, Tertiary, and Branched Alkanols, Cycloalkanols, Alkanediols, Alkanetriols, Ether Alkanols, and Aromatic Hydroxy Derivatives,” J. Chem. and Eng. Data, **42** (3), pp. 415-433.

[24] Cibulka, I., and Takagi, T., 1999, “P-ρ-T Data of Liquids: Summarization and Evaluation. 6. Nonaromatic Hydrocarbons (Cn, n ≥ 5) Except n-Alkanes C5 to C16,” J. Chem. and Eng. Data, **44** (6), pp. 1105–1128.

[25] Rogers, P.A., 1993, “Pressure–Volume–Temperature Relationships for Polymeric Liquids: A Review of Equations of State and their Characteristic Parameters for 56 Polymers,” J. Appl. Polymer Sci., **48** (6), pp. 1061-1080.

[26] Dymond, J.H., Malhotra, R., Isdale, J.D. and Glen, N.F.M., 1988, “(p, r, T) of n-Heptane, Toluene, and Oct-1-ene in the Range 298 to 373 K and 0.1 to 400 MPa and Representation by the Tait Equation,” J. Chem. Thermodyn., **20** (5), pp. 603-614.

[27] Fakhreddine, Y.A. and Zoller, P., 1990, "The Equation of State of a Polydimethylsiloxane Fluid", *J. Appl. Polymer Sci.*, **41**, pp.1087-1093.

[28] Habchi, W., Eyheramendy, D., Vergne, P. and Morales-Espejel, G., 2012, "Stabilized Fully-Coupled Finite Elements for Elastohydrodynamic Lubrication Problems," Adv. Eng. Softw., **46**, pp. 4-18.

[29] Yang, P., Wen, S., 1990, "A Generalized Reynolds Equation for Non-Newtonian Thermal Elastohydrodynamic Lubrication," ASME J. Tribol., **112**, pp. 631-636.

[30] Wu, S. R., 1986, "A Penalty Formulation and Numerical Approximation of the Reynolds-Hertz Problem of Elastohydrodynamic Lubrication," Int. J. Eng. Sci., **24** (6), pp. 1001-1013.

[31] Deuflhard, P., 2004, "Newton Methods for Nonlinear Problems, Affine Invariance and Adaptive Algorithms," Springer, Germany.

[32] Kleinschmidt, R.V., Bradbury, D. and Mark, M., 1953, "Viscosity and Density of Over Forty Lubricating Fluids of Known Composition at Pressures to 150,000 psi and Temperatures to 425 F," ASME, New York.

[33] Bair, S., 2009, "Rheology and High-Pressure Models for Quantitative Elastohydrodynamics," Proc. Inst. Mech. Eng., Part J: J. Eng. Tribol., **223** (4), pp. 617-628.

[34] Harris, K.R. and Bair, S., 2007, "Temperature and Pressure Dependence of the Viscosity of Di-isodecyl Phthalate at Temperatures between (0 and 100) °C and at Pressures to 1 GPa," *J. Chem. Eng. Data*, **52**, pp.272-278.

[35] Bair, S., 2002, "The High Pressure Rheology of Some Simple Model Hydrocarbons", Proc. Inst. Mech. Eng., Part J: J. Eng. Tribol., **216**, pp. 139-149.

[36] Bair, S., 2007, "High-Pressure Rheology for Quantitative Elastohydrodynamics," Elsevier Science, Amsterdam, pp.115-116, 225.

[37] Angell, C.A., 1995, "Formation of Glasses from Liquids and Biopolymers", *Science*, **276**, pp.1924-1935.

[38] Jubault, I., Molimard, J., Lubrecht, A. A., Mansot, J. L. and Vergne, P., 2003, "In Situ Pressure and Film Thickness Measurements in Rolling/Sliding Lubricated Point Contacts," Tribol. Lett., **15** (4), pp. 421-429.

[39] Van Leeuwen, H., 2009, "The Determination of the Pressure-Viscosity Coefficient of a Lubricant through an Accurate Film Thickness Formula and Accurate Film Thickness Measurements," Proc. Inst. Mech. Eng., Part J: J. Eng. Tribol., **223** (4), pp. 1143-1163.

[40] Krupka, I, Bair, S., Kumar, P., Khonsari, M. M. and Hartl, M., 2009, **"**An Experimental Validation of the Recently Discovered Scale Effect in Generalized Newtonian EHL," Tribol. Lett., **33**, 127-135.

[41] Lemmon, E.W., McLinden, M.O. and Friend, D.G., 2012, "Thermophysical Properties of Fluid Systems", NIST Chemistry WebBook, NIST Standard Reference Database Number 69, Eds. P.J. Linstrom and W.G. Mallard, National Institute of Standards and Technology, Gaithersburg MD, 20899.